JACS
JOURNAL OF THE AMERICAN CHEMICAL SOCIETY
Article
pubs.acs.org/JACS

A Hybrid Macrocycle with a Pyridine Subunit Displays Aromatic Character upon Uranyl Cation Complexation

I-Ting Ho,[†,∥] Zhan Zhang,[†,∥] Masatoshi Ishida,*[,‡] Vincent M. Lynch,[†] Won-Young Cha,[§] Young Mo Sung,[§] Dongho Kim,*[,§] and Jonathan L. Sessler*[,†]

[†]Department of Chemistry, The University of Texas at Austin, 105 East 24th Street, Stop A5300, Austin, Texas 78712-1224 United States

[‡]Education Center for Global Leaders in Molecular Systems for Devices, Kyushu University, Fukuoka 819-0395, Japan

[§]Department of Chemistry, Yonsei University, Seoul 120-749, Korea

Supporting Information

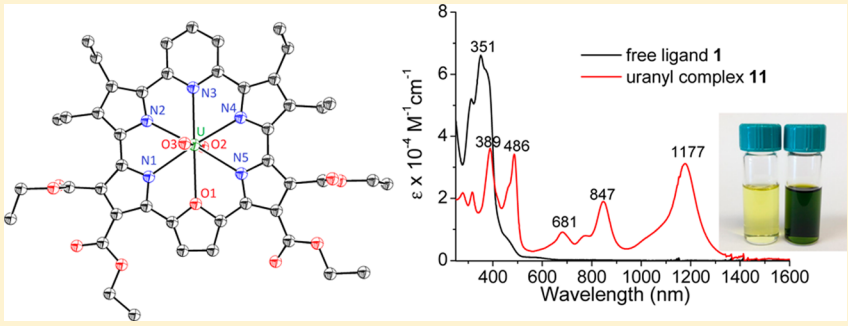

ABSTRACT: Reported here is a new hybrid macrocycle, cyclo[1]furan[1]pyridine[4]pyrrole (**1**), that bears analogy to the previously reported mixed heterocycle system cyclo[2]pyridine[4]pyrrole (**2**) and cyclo[6]pyrrole **3**, an all-pyrrole 22 π-electron aromatic expanded porphyrin. The oxidized, dianionic form of **1**, $[\mathbf{1} - 4H]^{2-}$, has been characterized as its uranyl complex. In contrast to **2** and **3** and in spite of the presence of a 2,6-disubstituted pyridine subunit, the uranyl complex of $[\mathbf{1} - 4H]^{2-}$ displays solid-state structural and solution-phase spectroscopic features consistent with contributions to the overall electronic structure that involve a conjugated, $(4n + 2)$ π-electron aromatic periphery.

INTRODUCTION

Expanded porphyrins have been used extensively in recent years to study aromaticity and antiaromaticity effects because of their distinctive optical and electrochemical features.[1] 2,5-Disubstituted pyrrole, the key subunit in most expanded porphyrin systems, as well as in synthetic and naturally occurring porphyrins, has played a central role in these efforts. This is because it allows through conjugation in both its normal reduced and oxidized states (cf. Figure 1). Moreover, the loss and gain of the pyrrole NH proton that accompany oxidation and reduction, respectively, often allow conjugated expanded porphyrins to access different electronic states (e.g., aromatic $(4n + 2)$- and antiaromatic $4n$ π-electron forms) without a net change in the charge of the macrocycle. The behavior of 2,5-disubstituted pyrroles stands in marked contrast to that of 2,6-disubstituted pyridines. These latter heterocycles do not permit through conjugation without loss of local aromaticity (Figure 1).

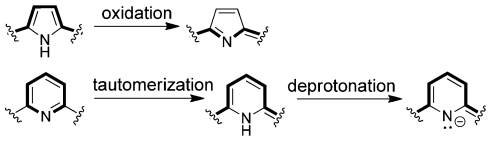

Figure 1. Schematic representation of cross conjugation in reduced and oxidized 2,5-disubstituted pyrroles and the loss of local aromaticity that typically precludes through conjugation in the case of 2,6-disubstituted pyridines.

As a result, a pyridine as a subunit for the construction of fully conjugated macrocycles is still rare. Breitmaier and co-workers initially attempted to synthesize an 18 π-electron aromatic pyriporphyrin; however, unexpected products, dimeric porphyrin and pyriporphyrinone, were obtained.[2] Lash and co-workers first reported an aromatic pyriporphyrin containing an embedded 3-hydroxypyridine, where the keto−enol tautomerization allowed stabilization of the proposed 18 π-electron aromatic periphery.[3] Later, they synthesized an aromatic pyriporphyrin wherein a CO_2Ph protective group is attached to the inverted pyridine nitrogen.[4] These advances not withstanding, pyriporphyrins containing unsubstituted pyridines incorporated within a bona fide aromatic periphery remain all but unknown.[5,6] On the other hand, if strategies were

Received: December 15, 2013
Published: February 25, 2014

dx.doi.org/10.1021/ja412520g | J. Am. Chem. Soc. 2014, 136, 4281−4286

developed that allowed pyridine subunits to be incorporated into conjugated macrocycles, they might permit the rich lexicon of porphyrin analogues to be expanded further. With this view in mind, we recently prepared the cyclo[2]pyridine[4]pyrrole **2**,[7] an analogue of the all-pyrrole 22 π-electron aromatic expanded porphyrin cyclo[6]pyrrole **3**.[8] As inferred from theoretical studies, nucleus-independent chemical shift (NICS)[9] calculations, and spectroscopic analyses, the dicationic form $[\mathbf{2} + 2H]^{2+}$ permits electronic communication through the pyridine subunits, thus imparting electronically delocalized 24 π-electron antiaromatic character to the system as a whole (Figure 2a). Separately, Lash and co-workers reported that the

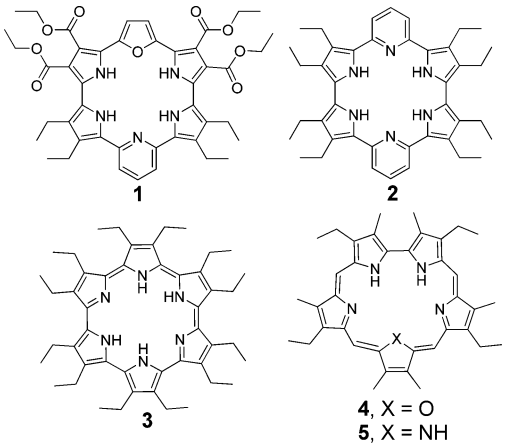

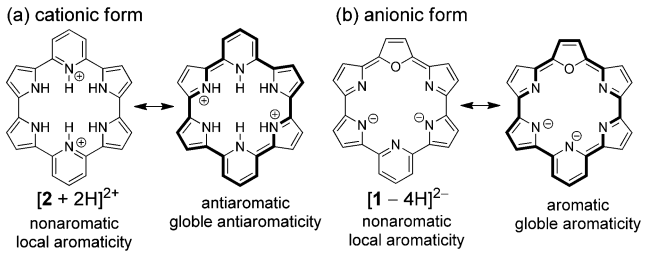

Figure 2. Chemical representations of various expanded porphyrins. Resonance structures of (a) the cationic species $[\mathbf{2} + 2H]^{2+}$ and (b) the oxidized, anionic form $[\mathbf{1} - 4H]^{2-}$ of the mixed furan–pyridine–pyrrole macrocycle **1**, which is the subject of the present study. Substituents on pyrrole rings have been removed for clarity.

protonated form of a 6-oxopyriphlorin displayed weakly diatropic character, a finding that was attributed to an 18 π-electron delocalized resonance contributor.[5]

As an alternative to protonation, we envisioned that the anionic form of pyridine might also allow for electronic delocalization within a conjugated macrocycle (Figure 2b). To the best of our knowledge, this approach has yet to be exploited to create a pyridine-containing expanded porphyrin with aromatic character. However, recently, Neya and co-workers suggested that the nickel complex of pyricorrole, a trispyrrole, monopyridine-containing porphyrin analogue, was stabilized as the result of an 18 π-electron aromatic periphery.[6] This conclusion was based on the observation of a modest downfield shift for the pyridine proton signals in the ^{1}H NMR spectrum, the presence of a weak Q-like band in the UV–vis absorption spectrum, and bond length asymmetry in the solid-state structure. However, no supporting calculations were presented. Moreover, the corresponding metal-free (and presumably nonaromatic) form of the macrocycle was not reported. Therefore, the extent of aromatic character (if any) could not be quantified. Here, we report a new hybrid macrocycle, cyclo[1]furan[1]pyridine[4]pyrrole **1**, and show that its dianionic form $[\mathbf{1} - 4H]^{2-}$ may be stabilized as its uranyl complex. As detailed below, this latter complex, but not the metal-free, neutral macrocycle, displays spectroscopic features consistent with contributions to the overall electronic structure that include a conjugated, $(4n + 2)$ π-electron aromatic periphery.

The uranyl cation (UO_2^{2+}) was chosen as the Lewis acidic center to stabilize the putative dianionic form of **1** because of its stability in a hexagonal planar coordination environment and because it was expected to be of an appropriate size to be accommodated within the macrocycle cavity. Moreover, prior studies had served to show that the insertion of the uranium(VI) cation into expanded porphyrins could lead to changes in the oxidation state and hence overall electron count of the annulene-like periphery.[10−12] For instance, cyclo[6]-pyrrole **3**, an aromatic species containing a 22 π-electron periphery in its metal-free form, was found to undergo oxidation upon uranyl cation complexation, giving rise to a formally 20 π-electron antiaromatic heteroannulene.[10] In this case, metal insertion leads to bleaching of the spectral features. On the other hand, complexation of the uranyl cation by **1** would be expected to lead to a dramatic increase in spectral intensity in the event that aromatic character was being developed. As detailed below, this indeed proved to be the case; in fact, a dark green complex is produced from a light yellow precursor.

RESULTS AND DISCUSSION

On the basis of the analogy between **2** and **3**, we considered it likely that the bispyridine system **2** could be used to prepare a stable uranyl complex using the same metal insertion methods employed in the case of **3**. However, initial studies failed to yield promising results. Therefore, one pyridyl subunit was replaced synthetically by a furan subunit. This replacement was driven by the early observation that oxasapphyrin **4**[13] (a monofuran, tetrapyrrolic macrocycle), in contrast to sapphyrin **5**[14] (a pentapyrrolic expanded porphyrin), readily formed a stable uranyl complex.

The synthesis of macrocycle **1** is shown in Scheme 1. The target compound **1** was constructed from two principle building blocks, namely, the dibromo-2,5-dipyrrolylfuran **9** and the diborate-functionalized 2,6-dipyrrolylpyridine **10**. Precursor **9** was prepared, in turn, from pyrrole **6**.[15] Reaction of **6** with NBS at 0 °C in an ice bath provided the monobrominated product **7** in 60% yield. Subsequent Suzuki coupling with dipinacolborate furan in the presence of $Pd(dppf)Cl_2$ and K_2CO_3 in DMF/H_2O yielded the 2,5-dipyrrolylfuran **8** in 28% yield. Bromination then gave **9** in 68% yield. 2,6-Dipyrrolylpyridine diborate **10** was synthesized as previously reported by our group.[7] $Pd(dppf)Cl_2$-catalyzed Suzuki coupling of **9** and **10** produced the target macrocycle **1** in 30% isolated yield under conditions of slow addition. All new compounds were characterized by ^{1}H and ^{13}C NMR spectroscopy and by HRMS (see the Experimental Section in the Supporting Information). Macrocycle **1** was found to have poor solubility in CH_2Cl_2, $CHCl_3$, and CH_3CN. However, it could be dissolved readily in acetone and DMSO.

A single crystal of **1** suitable for X-ray diffraction analysis was grown from a mixture of DMSO and CH_2Cl_2. The resulting structure is shown in Figure 3. As can be seen from an

dx.doi.org/10.1021/ja412520g | J. Am. Chem. Soc. 2014, 136, 4281−4286

Scheme 1. Synthesis of Cyclo[1]furan[1]pyridine[4]pyrrole 1 and Its Uranyl Complex 11[a]

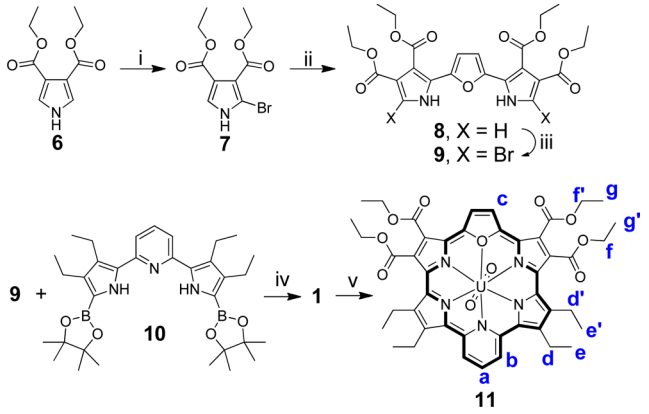

[a]Reagents and conditions: (i) NBS, THF, −78 to 0 °C, 60%; (ii) 2,5-bis(4,4,5,5-tetramethyl-1,3,2-dioxaborolan-2-yl)furan, $Pd(dppf)Cl_2$, K_2CO_3, DMF/H_2O, 95 °C for 20 h, 28%; (iii) NBS, THF, 0 °C for 2 h, 68%; (iv) $Pd(dppf)Cl_2$, K_2CO_3, DMF/H_2O, 95 °C for 20 h, 30%; (v) $UO_2[(Me_3Si)_2N]_2(THF)_2$, dry CH_2Cl_2, reflux for 24 h, 73%.

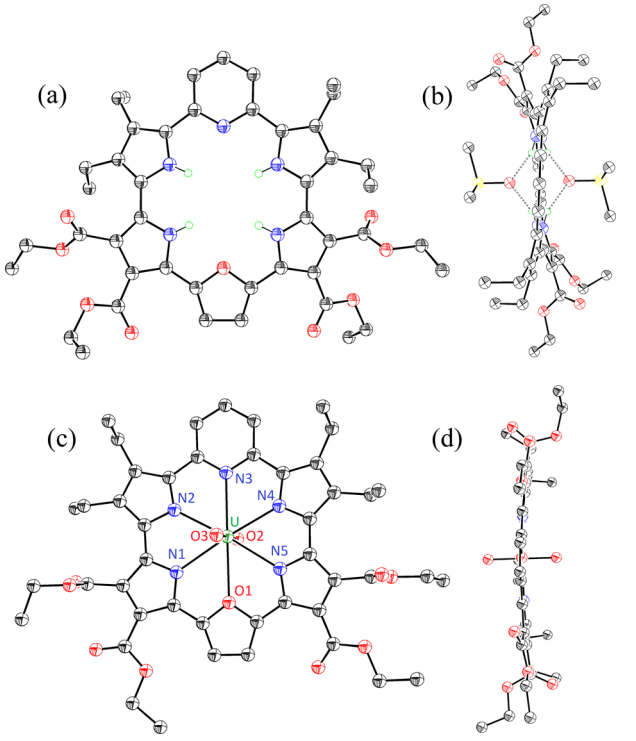

Figure 3. Single-crystal X-ray diffraction structures of **1** and the uranyl complex **11**: (a) top and (b) side views of **1** (the DMSO molecule is omitted for clarity from the top view); (c) top and (d) side views of **11**. All hydrogens are omitted for clarity.

inspection of this figure, the macrocycle is slightly distorted. This distortion is ascribed to the apparent hydrogen-bonding interactions between the pyrrole NH protons and the oxygen atoms of the two bound DMSO solvent molecules. Steric repulsion between the peripheral ester and ethyl groups also likely contributes to the observed deviation from planarity. The diagonal distance between the two nitrogen atoms of the pyrrole subunits is 5.181 Å, a value that is shorter than the corresponding distance in cyclo[6]pyrrole **3** (5.29 Å).[10] The cavity of **1** is thus slightly smaller than that in cyclo[6]pyrrole **3**. This was expected to make it even better suited for uranyl cation complexation.

In fact, the uranyl complex **11** could be obtained readily when **1** was reacted with $UO_2[(Me_3Si)N]_2THF_2$ in dry CH_2Cl_2 under anaerobic conditions (Scheme 1). After removal of the solvent and purification by column chromatography over aluminum oxide (CH_2Cl_2, eluent) under a normal laboratory atmosphere, the uranyl complex **11** was isolated as a dark green solid in 73% yield. In analogy to what proved true for **3**,[10] it is assumed that, during the course of metal insertion and workup, oxidation of the macrocycle occurs. To the extent that conjugation through the pyridine subunit is allowed, this would give rise to a system with 22 π-electron aromatic heteroannulene character.

Support for the proposed increase in conjugation came from spectroscopic studies. The UV−vis absorption spectrum of the metal-free system **1** (recorded in CH_2Cl_2) displays a major absorption band at 351 nm (ε = 66 000 dm^3 cm^{-1} mol^{-1}) (Figure 4). Macrocycle **1** also proved to be fluorescent and to

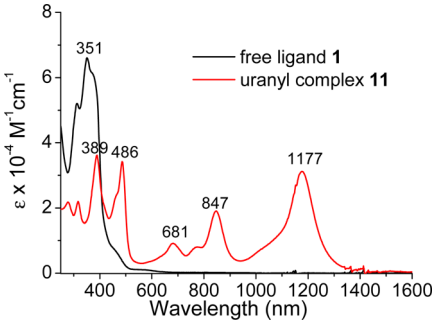

Figure 4. UV−vis−NIR absorption spectra of macrocycle **1** and its uranyl complex **11** recorded in CH_2Cl_2.

possess a long-lived excited singlet state, features that are consistent with a lack of aromaticity. In CH_2Cl_2, the excited state was found to decay in a biexponential fashion, with the two time components (830 ps and 6.4 ns) presumably reflecting the different conjugation segments within the macrocycle (Figure 5). In contrast, the spectrum of the uranyl complex **11** (in CH_2Cl_2) is characterized by two sharp Soret-like bands, at 389 (ε = 34 400) and 486 (32 400) nm, which are accompanied by three Q-like bands at 681 (8700), 847 (18 100), and 1177 (29 700) nm. The appearance of new, intense absorption bands at longer wavelengths is consistent with the

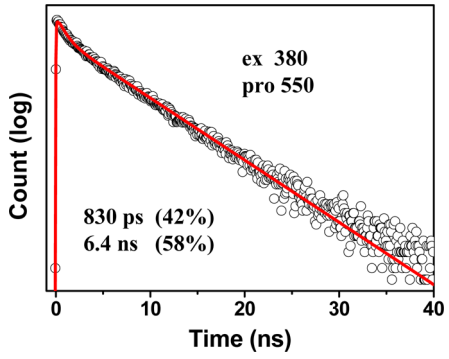

Figure 5. Fluorescence decay profile of **1** measured by time-correlated single-photon counting (TCSPC; excitation (ex) at 380 nm; probed (pro) at 550 nm).

dx.doi.org/10.1021/ja412520g | J. Am. Chem. Soc. 2014, 136, 4281−4286

suggestion that the extent of π-electron conjugation within the macrocycle increases upon metalation. In CH_2Cl_2, the uranyl complex **11** exhibits fast transient absorption (TA) decay dynamics. The decay profile of **11** probed at 1300 nm was well fitted by a monoexponential function with a time constant of 2.5 ps (Figure 6). These decay dynamics are consistent with the

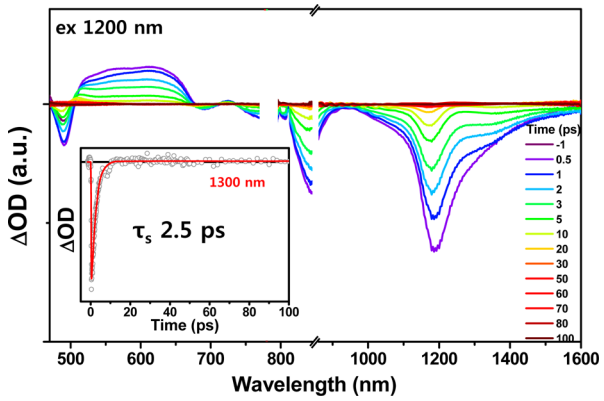

Figure 6. Transient absorption spectra and decay profile of **11** in CH_2Cl_2.

presence of a fully conjugated chromophore[16] whose excited singlet state decays rapidly as the result of a spin−orbit coupling enhancement produced by the presence of a coordinated heavy atom. To support this conclusion, an effort was made to record the triplet−triplet absorption spectrum of the uranyl complex **11** (cf. Figure S19, Supporting Information). No signals could be observed. This is as would be expected for uranyl complex **11**, which undergoes significantly fast intersystem crossing (ISC) and is subject to very fast ground-state recovery as the result of a heavy atom effect arising from the coordinated uranium(VI) cation.

Further support for the conclusion that the uranyl complex **11** possesses aromatic character came from ^{1}H NMR spectroscopic studies carried out in $CDCl_3/CD_3OD$ (20/1, v/v). As shown in Figure 7, the protons on the pyridine and furan subunits in macrocycle **1** were found to resonate in a region typical of what is seen for the isolated heterocycles, namely, between 7.00 and 8.00 ppm. In contrast, the protons on the pyridine and furan subunits in the uranyl complex **11** are shifted to significantly lower field ($\Delta\delta$ 2.08, 3.41, and 2.86 ppm for H_a, H_b, and H_c, respectively); they appear as well-defined

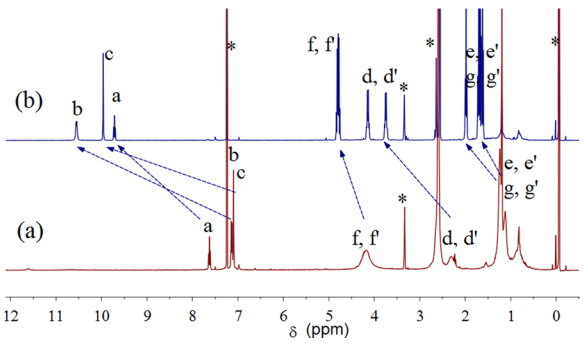

Figure 7. ^{1}H NMR spectra of (a) neutral macrocycle **1** and (b) complex **11** recorded in $CDCl_3/CD_3OD$ (20/1, v/v). Labels shown in the spectra correspond to those of Scheme 1. An asterisk designates residual protic solvents and TMS.

doublets and triplets, respectively. This downfield shift is consistent with the presence of a diatropic ring current within the macrocycle, as would be expected for a system with aromatic character.

The proposed structure of **11** was confirmed by a single-crystal X-ray diffraction analysis (Figure 3c,d). Crystals of **11** were grown from a $CHCl_3$ solution via the slow diffusion of MeOH. The uranyl complex adopts a hexagonal-bipyrimidal geometry. The uranium center sits within the near-planar macrocycle with a distance of 0.019 Å to the mean plane defined by the six central N and O atoms and is slightly shifted toward the pyrrole−pyridine−pyrrole subunit as inferred from the U−N3 (2.610 Å) and U−O1 (2.686 Å) bond lengths. The U−N3 bond length of 2.610 Å is quite close to the average U−N distance. In contrast, the bond to the oxygen atom of the furan subunit, at a distance of 2.686 Å (U−O1), is the longest metal−ligand distance seen in the complex. The U−O2 and U−O3 bond lengths (both 1.767 Å) are typical of those for a normal, unperturbed UO_2^{2+} unit.[10,11,17]

A comparison of the carbon−carbon (C−C) bond lengths in **1** and its uranyl complex **11** provides further evidence for the proposed global π-electron delocalization. The average $C_\beta-C_\beta$ bond length of the pyrroles of 1.426 Å in **1** is reduced to 1.383 Å in the uranyl complex **11**. Furthermore, within the furan fragment the C−C bond lengths are roughly equal ($C_\alpha-C_\beta$ = 1.388 and 1.381 Å; $C_\beta-C_\beta$ = 1.388 Å). The bonds connecting the heterocyclic units in **11** also show a decrease in length relative to those of **1**. For instance, the average length of the bonds between the pyridine and pyrrole subunits in **1**, 1.472 Å, decreases to 1.447 Å in **11** (cf. Figure S13, Supporting Information). The harmonic oscillator model of aromaticity (HOMA)[18] index of **11** (via the global π-conjugated circuit) is thus increased to 0.775 compared with that of 0.586 in the case of **1**. These findings are ascribed to delocalization of the π-electrons into adjacent heterocyclic subunits along with stabilization of a quinoid-like resonance structure.

Electrochemical analyses of the macrocycle **1** and its uranyl complex **11** were carried out using cyclic voltammetry (Figure 8). In the voltammogram of **1**, two one-electron oxidation waves were observed with $E_{1/2}$ values of 0.10 and 0.36 V with peak potential separations (E_p) of 0.08 and 0.10 V, respectively. The CV of **11** displayed six redox processes, which is similar to what is seen in the CV of cyclo[6]pyrrole **3**. The well-defined redox curves of **11** are consistent with the presence of a fully conjugated periphery. The two reversible one-electron oxidations observed at 0.34 V (E_p = 0.10 V) and 0.79 V (E_p = 0.09 V) and the two reversible one-electron reductions seen at −0.43 (E_p = 0.09 V) and −0.72 (E_p = 0.09 V) are attributed to redox processes involving the macrocycle ring. The energy difference between the first one-electron reduction and the first one-electron oxidation of 0.79 V is slightly higher than the difference of 0.70 V observed in the uranyl complex of cyclo[6]pyrrole **3**.

To support the interpretation of the electronic structures of **1** and **11**, density functional theory (DFT) calculations were carried out using the Gaussian 09 program. Initial geometry optimizations produced structures similar to those obtained via X-ray diffraction analysis (cf. Figure S20 in the Supporting Information). In particular, the uranyl complex of **11** was calculated to possess a highly planar structure with U═O bond lengths (1.773 Å) expected for a U(IV) uranyl complex. The free base form of **1** was found to be nonaromatic, as inferred from the NICS[9] value of +2.13 ppm determined at the center of

dx.doi.org/10.1021/ja412520g | J. Am. Chem. Soc. 2014, 136, 4281−4286

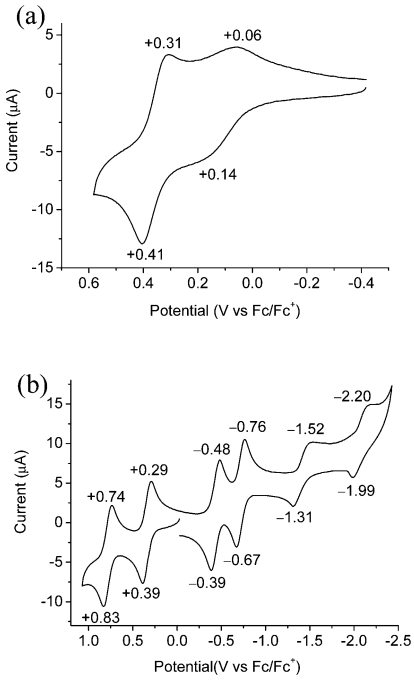

Figure 8. Cyclic voltamagrams of (a) **1** ([**1**] = 1 mM in 1% MeOH/CH_2Cl_2) and (b) **11** (CH_2Cl_2). The measurements were performed using a glassy carbon working electrode and a Pt counter electrode at a scan rate of 50 mV s^{-1} with 0.1 M TBA·PF_6 as the supporting electrolyte. Potentials are shown relative to that of ferrocene/ferrocenium.

the macrocycle. In contrast, the proposed aromatic character of **11** was supported by the anisotropy seen in the induced current density (AICD) plot,[19] which revealed a clockwise ring current as expected for a diatropic π-system (Figure 9a). Unfortunately, a reliable NICS value could not be obtained due to the presence of a heavy f-block uranyl cation at the center of the macrocycle. However, the downfield shifts for the $C_{(sp2)}$−H signals of the pyridine and furan rings of **11** computed assuming aromatic character were found to match those seen by experiment (Figure 9b). The same was true for the optical features (Figure 10). Moreover, using the $(4n + 2)$-electron perimeter model,[20] the number of nodal planes present in the π frontier molecular orbitals (MOs) of **11** was found to match those seen for 22-electron [20]annulenes (i.e., $[C_{20}H_{20}]^{2-}$).[12] We thus conclude that the complex **11** is a Hückel aromatic compound. The optical feature of the aromatic complex **11** could be predicted using the time-dependent (TD) DFT approach (Figure 10). Compared to the MO energy levels of **1**, the LUMO of the uranyl complex **11** is significantly stabilized, giving rise to a narrow HOMO−LUMO gap (Figures S21 and S22, Supporting Information). The lowest energy band (λ_{max} = 1177 nm) corresponds to the HOMO−LUMO transition at 1110 nm (f = 0.224). The other main bands consist of transitions from lower level HOMOs to the LUMO via some of the f-block metal-dominated LUMOs (e.g., LUMO + 1, LUMO + 2, LUMO + 3, etc.). Such findings are consistent with the fully conjugated electronic structure proposed for complex **11**.

The uranyl complex **11** was found to be stable when stored as a solid or in CH_2Cl_2 solution for prolonged periods of time at room temperature, as reflected by an absence of appreciable changes in the UV−vis spectrum over the course of 60 days. The stability of **11** under acidic conditions was also tested. This was done by recording the changes in spectral features as a

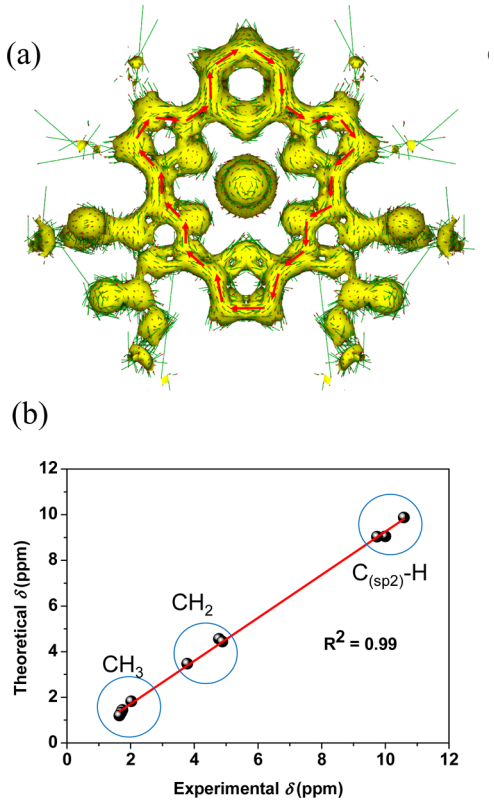

Figure 9. (a) AICD map at an isosurface value of 0.05 and (b) relationship between the computed screening constants δ and experimental values of **11**. The illustrated red vectors indicate the direction of the overall ring current when an external magnetic field is applied orthogonal to the macrocycle plane.

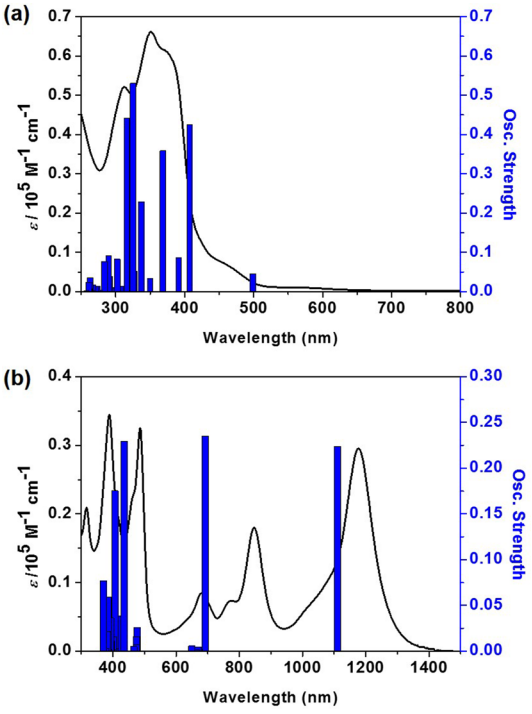

Figure 10. TD-DFT-computed vertical energies of (a) **1** and (b) **11** along with the experimental spectra.

function of time (Figure S15, Supporting Information). It was found that the uranyl complex (10 μM in CH_2Cl_2) underwent

dx.doi.org/10.1021/ja412520g | J. Am. Chem. Soc. 2014, 136, 4281−4286

nearly complete decomposition over the course of 22 days when allowed to stand at ambient temperature in the presence of 30 equiv of TFA.

To assess the stability of the uranium complex **11** in the presence of other metal ions, complex **11** was treated with various metal salts in CH_2Cl_2 and heated at reflux for 24 h. Among the eight different metal ion salts tested, appreciable changes in the absorption spectrum of **11** were observed only in the presence of $SnCl_2$, $CuCl_2$, and $Th(NO_3)_4$ (Figure S16, Supporting Information). The observed changes in spectroscopic features could reflect decomposition of the uranium complex or metal ion replacement or some combination thereof. Studies of the coordination chemistry features of macrocycle **1** are currently in progress.[21]

In summary, a new hybrid macrocycle, cyclo[1]furan[1]pyridine[4]pyrrole **1**, was prepared via Suzuki coupling. Treatment with a U(VI) source under anaerobic conditions with workup and purification carried out in a normal laboratory environment results in stabilization of the oxidized, anionic form of **1** (i.e., $[\mathbf{1} - 4H]^{2-}$) in the form of its uranyl complex **11**. Spectroscopic, electrochemical, and theoretical studies of this complex provide support for the proposal that macrocycle $[\mathbf{1} - 4H]^{2-}$ possesses 22 π-electron aromatic heteroannulene character. These findings lead us to suggest that when appropriately stabilized by cation complexation 2,6-disubstituted pyridine subunits can be used to stabilize aromatic and antiaromatic electronic configurations, thus allowing their use in creating new expanded porphyrins and other conjugated macrocyclic systems.

■ ASSOCIATED CONTENT

Supporting Information

Synthetic experimental procedures, additional spectroscopic information, structural data, theory calculations, and CIF data. This material is available free of charge via the Internet at http://pubs.acs.org.

■ AUTHOR INFORMATION

Corresponding Authors

ishida@molecular-device.kyushu-u.ac.jp
dongho@yonsei.ac.kr
sessler@cm.utexas.edu

Author Contributions

‖I-Ting Ho and Zhan Zhang contributed equally to this work.

Notes

The authors declare no competing financial interest.

■ ACKNOWLEDGMENTS

This work was supported by the U.S. Department of Energy (DOE) Office of Basic Energy Sciences (Grant DE-FG02-01ER15186 to J.L.S.), the Midcareer Researcher Program (Grant 2005-0093839 to D.K.) administered through the National Research Foundation of Korea (NRF) funded by the Ministry of Education, Science and Technology (MEST), and Grant-in-Aid for Research Activity Start-up (No. 25888017 to M.I.) from the Japanese Society for the Promotion of Science.

■ REFERENCES

(1) (a) Jasat, A.; Dolphin, D. *Chem. Rev.* **1997**, *97*, 2267−2340. (b) Sessler, J. L.; Seidel, D. *Angew. Chem., Int. Ed.* **2003**, *42*, 5134−5175. (c) Aihara, J.; Makino, M. *Org. Biomol. Chem.* **2010**, *8*, 261−266. (d) Ishida, M.; Shin, J.-Y.; Lim, J. M.; Lee, B. S.; Yoon, M.-C.; Koide, T.; Sessler, J. L.; Osuka, A.; Kim, D. *J. Am. Chem. Soc.* **2011**, *133*, 15533−15544. (e) Mori, H.; Tanaka, T.; Osuka, A. *J. Mater. Chem. C* **2013**, *1*, 2500−2519. (f) Yoneda, T.; Osuka, A. *Chem.—Eur. J.* **2013**, *19*, 7314−7318.

(2) Berlin, K.; Breitmaier, E. *Angew. Chem., Int. Ed. Engl.* **1994**, *33*, 219−220.

(3) Lash, T. D.; Chaney, S. T. *Chem.—Eur. J.* **1996**, *2*, 944−948.

(4) Lash, T. D.; Pokharel, K.; Serling, M. J.; Yant, V. R.; Ferrence, G. M. *Org. Lett.* **2007**, *9*, 2863−2866.

(5) Young, A. M.; Lash, T. D. *Org. Biomol. Chem.* **2013**, *11*, 6841−6848.

(6) Neya, S.; Suzuki, M.; Matsugae, T.; Hoshino, T. *Inorg. Chem.* **2012**, *51*, 3891−3895.

(7) Zhang, Z.; Lim, J. M.; Ishida, M.; Roznyatovskiy, V. V.; Lynch, V. M.; Gong, H.-Y.; Yang, X.; Kim, D.; Sessler, J. L. *J. Am. Chem. Soc.* **2012**, *134*, 4076−4079.

(8) Köhler, T.; Seidel, D.; Lynch, V.; Arp, F. O.; Ou, Z.; Kadish, K. M.; Sessler, J. L. *J. Am. Chem. Soc.* **2003**, *125*, 6872−6873.

(9) Chen, Z.; Wannere, C. S.; Corminboeuf, C.; Puchta, R.; Schleyer, P. v. R. *Chem. Rev.* **2005**, *105*, 3842−3888.

(10) Melfi, P. J.; Kim, S. K.; Lee, J. T; Bolze, F.; Seidel, D.; Lynch, V. M.; Veauthier, J. M.; Gaunt, A. J.; Neu, M. P.; Ou, Z.; Kadish, K. M.; Fukuzumi, S.; Ohkubo, K.; Sessler, J. L. *Inorg. Chem.* **2007**, *46*, 5143−5145.

(11) Sessler, J. L.; Seidel, D.; Vivian, A. E.; Lynch, V.; Scott, B. L.; Keogh, D. W. *Angew Chem., Int. Ed.* **2001**, *40*, 591−594.

(12) Furuyama, T.; Ogura, Y.; Yoza, K.; Kobayashi, N. *Angew Chem., Int. Ed.* **2012**, *51*, 11110−11114.

(13) Sessler, J. L.; Gebauer, A.; Hoehner, M. C.; Lynch, V. *Chem. Commun.* **1998**, 1835−1836.

(14) Burrell, A. K.; Cyr, M. C.; Lynch, V.; Sessler, J. L. *J. Chem. Soc., Chem. Commun.* **1991**, 1710−1713.

(15) Bush, L. C.; Heath, R. B.; Feng, X. U.; Wang, P. A.; Maksimovic, L.; Song, A. I.; Chung, W.-S.; Berinstain, A. B.; Scaiano, J. C.; Berson, J. A. *J. Am. Chem. Soc.* **1997**, *119*, 1406−1415.

(16) (a) Detty, M. R.; Merkel, P. B. *J. Am. Chem. Soc.* **1990**, *112*, 3845−3855. (b) Ohulchanskyy, T. Y.; Donnelly, D. J.; Detty, M. R.; Prasad, P. N. *J. Phys. Chem. B* **2004**, *108*, 8668−8672. (c) Yoon, M.-C.; Misra, R.; Yoon, Z. S.; Kim, K. S.; Lim, J. M.; Chandrashekar, T. K.; Kim, D. *J. Phys. Chem. B* **2008**, *112*, 6900−6905.

(17) Sessler, J. L.; Vivian, A. E.; Seidel, D.; Burrell, A. K.; Hoehner, M.; Mody, T. D.; Gebauer, A.; Weghorn, S. J.; Lynch, V. *Coord. Chem. Rev.* **2001**, *216−217*, 411−434.

(18) Krygowski, T. M. *J. Chem. Inf. Comput. Sci.* **1993**, *33*, 70−78.

(19) Geuenich, D.; Hess, K.; Köhler, F.; Herges, R. *Chem. Rev.* **2005**, *105*, 3758−3772.

(20) (a) Michl, J. *J. Am. Chem. Soc.* **1978**, *100*, 6801−6811. (b) Michl, J. *J. Am. Chem. Soc.* **1978**, *100*, 6812−6818. (c) Michl, J. *J. Am. Chem. Soc.* **1978**, *100*, 6819−6824.

(21) Preliminary studies reveal that the addition of $SnCl_2$ and $Th(NO_3)_4$ to complex **11** in organic media serves to displace the coordinated uranyl cation from the macrocyclic core. The resulting putative metal-free macrocycle (a dianion) is, however, unstable and undergoes decomposition. On the other hand, on the basis of UV−vis and mass spectrometric analyses, exposure of **11** or the starting macrocycle **1** to $CuCl_2$ provided evidence of reaction, as inferred from UV−vis spectroscopic analyses (Figure S17, Supporting Information) and mass spectrometric studies (presence of peaks ascribable to $[\mathbf{1} + Cu]^+$ and $[\mathbf{1} + 2Cu]^+$; cf. Figure S18, Supporting Information). Efforts to isolate and characterize the resulting proposed complexes are ongoing.